

Journal of Mechanics of Materials and Structures

**FULLY PERIODIC RVES FOR TECHNOLOGICAL RELEVANT COMPOSITES:
NOT WORTH THE EFFORT!**

Konrad Schneider, Benjamin Klusemann and Swantje Bargmann

Volume 12, No. 4

July 2017



FULLY PERIODIC RVES FOR TECHNOLOGICAL RELEVANT COMPOSITES: NOT WORTH THE EFFORT!

KONRAD SCHNEIDER, BENJAMIN KLUSEMANN AND SWANTJE BARGMANN

The setup of a finite element model for homogenization featuring a fully periodic geometry and a fully periodic mesh topology in combination with a high quality discretization is a cumbersome task and might significantly reduce the overall efficiency in multiscale finite element simulations.

In this work, we examine multiple methodologies of setting up finite element models for homogenization purposes that extenuate these difficulties. Approaches resulting in periodic and nonperiodic representative volume element topologies in the microstructural generation process are introduced. Furthermore, we review and analyze various types of boundary conditions that either enforce periodicity or do not require periodicity of the underlying discretization. Approximate periodic boundary conditions are discussed in detail.

The benchmark study proves that a fully periodic topology and mesh discretization with periodic boundary conditions is not necessary in order to identify effective macroscopic material parameters for technologically relevant composites.

1. Introduction — numerical homogenization of heterogeneous solids

Advanced and complex materials often possess a distinctive microstructure at a certain length scale, which significantly influences the macroscopic material behavior. In composites, the combination of multiple material phases enhances mechanical properties over the single constituents, which in turn qualifies them as highly technologically relevant.

In computational micromechanics, the state of the art approach only considers a small but representative part of the structure, namely a representative volume element (RVE), featuring all relevant characteristics of the materials microstructure [Böhm 1998; Geers et al. 2010; Klusemann et al. 2012; Kari et al. 2007; McBride et al. 2012; Saeb et al. 2016; Schröder and Hackl 2014; Yuan and Fish 2008; Suquet 1985]. Such a RVE should have a sufficiently large size to capture enough microstructural information while being significantly smaller than the macroscopic structure to hardly influence macroscopic gradients [Böhm 1998].

One important issue to deal with is the application of appropriate boundary conditions. They have to be chosen carefully to fulfill the macrohomogeneity condition [Hill 1963] (also named the Hill–Mandel condition) for proper homogenization. At least five conditions obey this requirement: fully prescribed deformation over the entire domain, fully prescribed displacement on the boundary of the domain, periodic boundary conditions, fully prescribed stress vectors on the boundary of the domain and fully prescribed stresses over the entire domain.

Keywords: periodic boundary conditions, representative volume element, homogenization.

Secondly, application of the finite element method (FEM) requires a discretization of the RVE. The type and accuracy of such discretizations significantly influence the quality of the results. As will be shown in this work, periodic RVEs with periodic boundary conditions are not necessarily worth the effort.

In the opinion of many researchers, a favorable FE model features a periodic topology with a large number of inhomogeneities as well as high quality discretizations suitable for the direct application of periodic boundary conditions [Böhm 1998; Torquato 2002; Yue and E 2007; Kanit et al. 2003; Perić et al. 2011; Miehe and Koch 2002; Glüge 2013; Gusev 1997; Böhm and Han 2001; Böhm et al. 2002; Gitman et al. 2007]. The construction of such models is either a very tedious and expensive task or even impossible to accomplish for certain microstructures [Dirrenberger et al. 2014; Fritzen et al. 2009; Fritzen and Böhlke 2011].

Tremendous effort might be necessary to gather microstructural information and transfer it to a discretized model. If periodicity in terms of geometry and boundary conditions is targeted, this effort is questionable for engineering applications. Various possibilities of relaxing these strict requirements are possible to ease the homogenization procedure. Discretizing geometrically complex microstructures (e.g., curved geometric entities) is typically realized by employing tetrahedralizations. To achieve trustworthy analyses, high quality meshes are required; however, their generation might become a very cumbersome and resource consuming task [Böhm et al. 2002; Fritzen et al. 2009; Schneider et al. 2016]. A viable solution is the utilization of voxel discretizations resulting in regular grid-like meshes [Glüge 2013; Kanit et al. 2003]. Regular voxel meshes naturally feature a periodic mesh topology, allowing a straightforward application of periodic boundary conditions.

As an alternative approach, approximate periodic boundary conditions and kinematic uniform stress vectors or displacement boundary conditions loosen the requirement of a periodic mesh topology. In fact, these methodologies allow completely nonperiodic RVEs.

The goal of this paper is a systematic evaluation of the influences of RVE topology, discretization and employed boundary conditions on the effective material response. A benchmark study is conducted for the example of composites consisting of a topologically interconnected matrix and nonoverlapping inclusions, so-called matrix inclusion composites.

2. Aspects of numerical homogenization in context of RVE topology, discretization and boundary conditions

Vital to a proper homogenization is the fulfillment of the macrohomogeneity condition suggested by Hill [1963]: the equality of the stress power deduced by the mean values (pure macroscopic quantities) and the stress power calculated by the actual volume integral of the microscopic quantities:¹

$$\bar{\mathbf{P}} : \dot{\bar{\mathbf{F}}} = \frac{1}{V_0} \int_{\mathcal{B}_0} \mathbf{P} : \dot{\mathbf{F}} \, dV_0. \quad (1)$$

Here, V_0 is the volume in the reference configuration, \mathbf{P} represents the first Piola–Kirchhoff stress tensor and \mathbf{F} is the deformation gradient. The fulfillment is accomplished by the proper choice of boundary conditions.

¹Quantities on the macroscopic scale are related to the microscopic scale via a volume average over the RVE domain \mathcal{B}_0 and are denoted by $\overline{(\dots)} = 1/V_0 \int_{\mathcal{B}_0} (\dots) \, dV_0$ in the following. Accordingly, the macroscopic deformation gradient is introduced via $\bar{\mathbf{F}} = 1/V_0 \int_{\mathcal{B}_0} \mathbf{F} \, dV_0$.

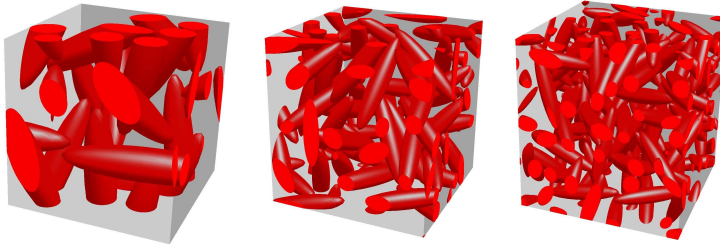


Figure 1. Example microstructures for an inclusion volume fraction of $f = 20\%$ featuring a periodic topology with (left) 10 inclusions, (center) 50 inclusions and (right) 100 inclusions.

2.1. Microstructure generation. In the following, the underlying RVE geometry is exemplarily based on matrix-inclusion microstructures.

The key idea of a RVE with an a priori periodic topology is approximating inhomogeneous materials by infinitely extended model materials with a periodic phase arrangement [Michel et al. 1999]. The constraint of generating a fully periodic geometry results in additional effort.

The generation process is based on our random sequential adsorption algorithm [Schneider et al. 2016]. Inclusions are modeled as nonoverlapping spheroids randomly orientated and located inside a cubic RVE as depicted in Figure 1. All investigated RVEs feature a target inclusion volume fraction of $f = 20\%$ with equally shaped, nonoverlapping spheroids incorporating an aspect ratio of $\gamma = \frac{1}{5}$ (ratio of minor to major spheroid axis).²

The size of the RVE is triggered by the ratio of the characteristic length of the microstructural components l (major axis of a spheroid) and the RVE edge length d . Three setups of 10, 50 and 100 inclusions along with their respective ratios, listed in Table 1, are considered.^{3 4}

target inclusion number	n	10	50	100
major spheroid axis (l) / RVE length (d)	l/d	0.49	0.28	0.23

Table 1. Ratios of characteristic lengths of microstructural components l (longest axis of the spheroid) and RVE dimension d for target inclusions numbers of 10, 50 and 100.

²Periodic RVEs always exhibit this intended inclusion volume fraction since a placed inclusion intersecting the RVE boundary has its periodic counterparts also inside the RVE. However, the actual volume fractions of inclusions intersecting with the RVE boundary cannot be determined exactly in advance due to the random nature of the placement procedure. Therefore, the inclusion volume fraction for nonperiodic cases are only approximate. The actual microstructure generation process for the nonperiodic case is terminated, if the inclusion volume fraction deviates less than 1% from target volume fraction.

³ A RVE with a nonperiodic topology typically contains more inclusions than its periodic counterpart: randomly placed inclusions intersecting the RVEs boundary do not have periodic continuations and, thus, more inclusions are required to achieve the preassigned inclusion volume fraction.

⁴The expression l/d converges towards zero with an increasing inclusion number as the RVE length is set to $d = 1$ and remains constant. In the limit of infinitely many inclusions, $l \rightarrow 0$ and, thus, $l/d \rightarrow 0$.

2.2. FE discretizations. Two element types are employed for three-dimensional discretizations, namely tetrahedral or hexahedral elements. Tetrahedral elements are more versatile in terms of meshing complicated geometries, but typically exhibit increased computational costs compared to hexahedral elements [Benzley et al. 1995; Carl et al. 2006].

An alternative to avoid the tedious task of precisely resolving the geometry via a sophisticated mesh represents the utilization of fully structured grids, also known as voxel discretization. By assigning each element to material phases by means of the location of element midpoints or even Gauss points, it is possible to capture the geometric features to a certain extent. As a consequence, the mesh is easily generated, see Figures 2 and 3.

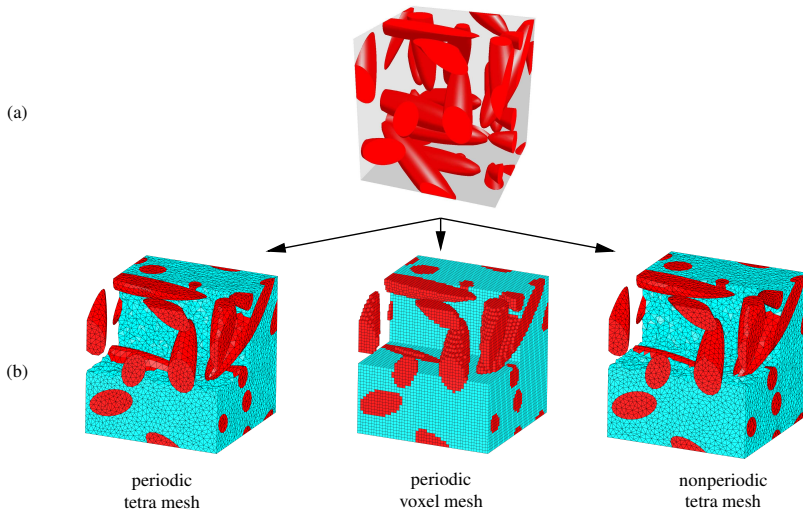


Figure 2. Periodic model setups considered in this study: (a) periodic topology and (b) tetrahedral and voxel discretizations.

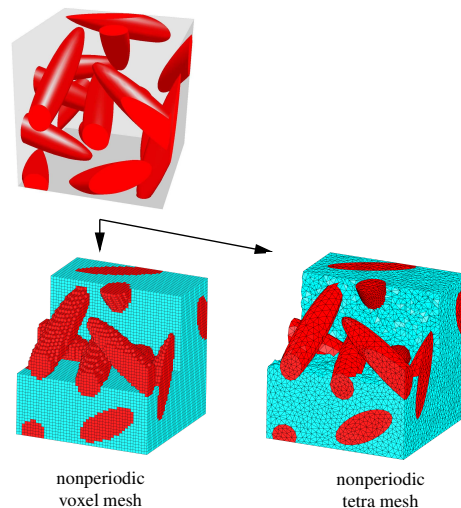


Figure 3. Nonperiodic model setups considered in this study: (a) nonperiodic topology and (b) tetrahedral and voxel discretizations.

We consider quadratic tetrahedral meshes as well as voxel discretizations featuring linear hexahedral elements. In this context, a tetrahedralization of the geometry generally provides higher geometric accuracy. However, due to the sharp curvature of the inclusions, the geometry cannot be perfectly captured. Following [Schneider et al. 2016], constrained triangulations and tetrahedralizations are utilized to generate high quality meshes which possess periodicity.

2.3. Boundary conditions. By applying boundary conditions to the RVE, macroscopic loadings are transferred to the microscale. Typically, the macroscopic deformation gradient $\bar{\mathbf{F}}$ or the macroscopic first Piola–Kirchhoff stress tensor $\bar{\mathbf{P}}$ are imposed on the microfield.

Kinematic uniform boundary conditions are formulated for the displacements \mathbf{u} on the entire boundary $\partial\mathcal{B}_0$ of the RVE via

$$\mathbf{u} = \bar{\mathbf{F}} \cdot \mathbf{X} \quad \forall \mathbf{X} \in \partial\mathcal{B}_0. \quad (2)$$

Here, \mathbf{X} denotes the position vector of a material point in the reference configuration of the RVE. Since the displacements are fully prescribed on the entire boundary, this boundary condition does not have any requirements on the mesh topology, making it operationally very easy to implement. Disadvantageously, the macroscopic response is predicted to be too stiff, resulting from strongly restricted degrees of freedom [Pecullan et al. 1999; Miehe and Koch 2002; Kanit et al. 2003].

Periodic boundary conditions relax these kinematic constraints. The boundary of the RVE is split into associated parts $\partial\mathcal{B}_0 = \partial\mathcal{B}_0^+ \cup \partial\mathcal{B}_0^-$ with associated material points \mathbf{X}^+ and \mathbf{X}^- . Displacements show a periodic behavior, whereas the tractions \mathbf{p} are antiperiodic:

$$\begin{aligned} \mathbf{u}(\mathbf{X}^+) - \mathbf{u}(\mathbf{X}^-) &= [\bar{\mathbf{F}} - \mathbf{1}] \cdot [\mathbf{X}^+ - \mathbf{X}^-] \text{ and} \\ \mathbf{p}(\mathbf{X}^+) + \mathbf{p}(\mathbf{X}^-) &= \mathbf{0} \quad \forall \mathbf{X}^+, \mathbf{X}^- \in \partial\mathcal{B}_0^+, \partial\mathcal{B}_0^-. \end{aligned} \quad (3)$$

Since the boundary is divided into opposing (periodic) counterparts, it is an inevitable requirement for the underlying discretization to possess a periodic mesh topology.

Furthermore, static uniform boundary conditions:

$$\mathbf{t} = \bar{\mathbf{P}} \cdot \mathbf{N} \quad \forall \mathbf{N} \in \partial\mathcal{B}_0 \quad (4)$$

are considered. Here, \mathbf{t} represents the stress vector in the current configuration and \mathbf{N} is the normal vector of the boundary in the reference configuration. Static uniform boundary conditions do not have any requirements on the mesh. Difficulties concerning the uniqueness of a solution resulting from the pure Neumann problem are overcome by employing *semi-Dirichlet boundary conditions* as suggested in [Javili et al. 2017; Saeb et al. 2016]. Rigid body motions are restricted by fixing one corner node in all three coordinate directions and applying *semi-Dirichlet boundary conditions* to the other corner nodes.⁵

2.3.1. Approximate periodic boundary conditions (APBC). If the underlying mesh topology is not periodic, there is no straightforward way to apply periodic boundary conditions. To circumvent the restriction on the mesh topology, some researchers weakly impose periodic boundary conditions on a nonperiodic mesh [Larsson et al. 2011; Nguyen et al. 2012; Xia et al. 2003]. However, these methods demand sophisticated programming and are hardly applicable to commercial software. A more practical approach

⁵Within the commercial FE software package Abaqus, static uniform boundary conditions are implemented via the DLOAD option.

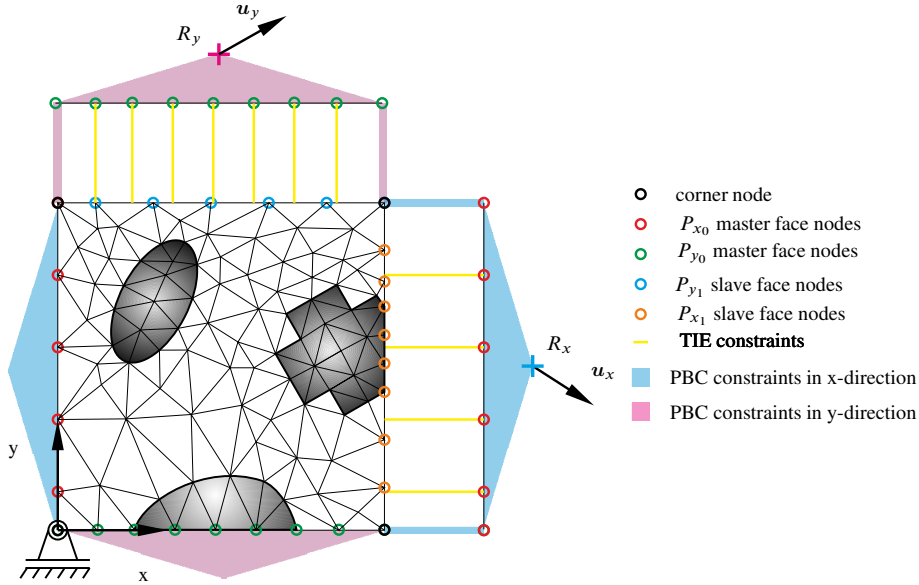


Figure 4. Sketch of approximate periodic boundary conditions using surface-to-surface constraints (e.g., TIE-constraints in Abaqus).

(suggested in [Yuan and Fish 2008; Kassem 2009]) is to apply approximate periodic boundary conditions via surface-to-surface constraints, available in commercial FE software packages, e.g., in Abaqus.

A schematic illustration of this method for the two-dimensional case is depicted in Figure 4. First, master faces $P_{x_0} : X = 0$ (red nodes) and $P_{y_0} : Y = 0$ (green nodes) are introduced. These faces are copied and, for better illustration purposes, translated to their opposing counterparts, namely $P_{x_1} : X = l_x$ (orange nodes) and $P_{y_1} : Y = l_y$ (blue nodes), with l_x and l_y being the dimensions of the RVE. The required constraints for the periodic boundary conditions are then formulated between reference points (R_x and R_y), copied faces and their source faces. Therefore, identical nodal distributions are maintained a priori, see the blue and violet area in Figure 4. Furthermore, the actual RVE boundaries P_{x_1} and P_{y_1} are coupled to the copied faces via surface-to-surface coupling, thus consequently equalizing their motion respectively and tying them together.⁶ During this coupling, P_{x_1} and P_{y_1} act as slave surfaces implying the condensation of degrees of freedom of associated nodes.

In Abaqus, an element-based master-slave surface algorithm is employed. To every point on the master surface, the closest nodes on the slave surface are computed by a projection procedure. These quantities are then coupled via constraints which are generated using the element shape functions.

Special care must be taken to set up constraints for the corners (black nodes) and edges (in three dimensions) of copied surfaces to circumvent overconstraining. Edges and corner nodes are excluded in the coupling process and are processed via separate multipoint constraints. In particular, three master edges ($L_{x_0y_0} : x = y = 0$, $L_{y_0z_0} : y = z = 0$, $L_{x_0z_0} : x = z = 0$) have to be introduced and copied for

⁶As a consequence, all involved surfaces show the same motion during an analysis. In Abaqus, this coupling is conveniently established by utilizing the *TIE keyword.

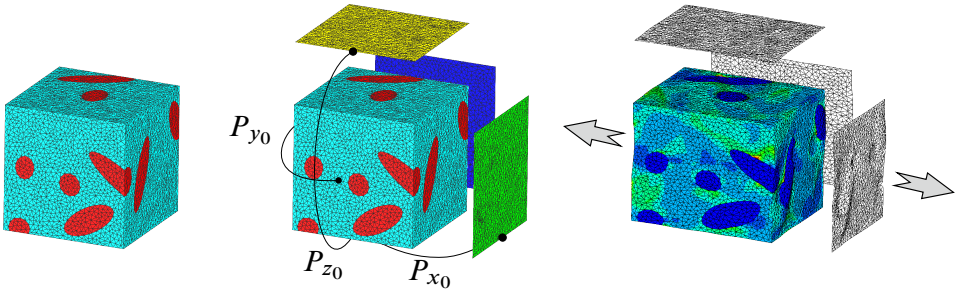


Figure 5. Model setup for a 3d nonperiodic mesh topology using TIE-constraints: virgin mesh (left), TIE-constraints with copied P_{x_0} , P_{y_0} and P_{z_0} faces (center) and conducted analysis for tensile loading (right).

coupling to each slave edge (analogously to the mentioned surfaces).⁷ Since edges are one-dimensional, a coupling solely relying on nodal distributions is utilized.⁸ The displacements are prescribed at the reference nodes before analysis.

Following the described approach, we are able to apply approximate periodic boundary conditions to nonperiodic three-dimensional meshes. Figure 5 exemplarily depicts a three-dimensional nonperiodic model. An additional investigation of the approximate periodic boundary conditions can be found in the Appendix.

3. Numerical examples

3.1. Set-up of benchmark study. All RVEs have a unit edge length d whereas the spheroid axis length l varies to trigger the RVE size. For each RVE, 20 randomized realizations are considered. A statistical study is given to support the results and extenuate artificial findings due to the randomness of the RVE generation process. To this end, a total of 3600 simulations are conducted for this study.⁹ Two oppositional cases of matrix-inclusion materials are investigated:

- (i) materials with soft inclusions and a stiff matrix, i.e., a low stiffness ratio $\alpha = E_{\text{Inclusion}}/E_{\text{Matrix}} = G_{\text{Inclusion}}/G_{\text{Matrix}}$ such as the polymer blend Acrylonitrile-Butadien-Styrene (ABS) [Michler 1992; Lombardo et al. 1994];
- (ii) materials with a very high stiffness ratio such as glass-fiber or carbon-fiber reinforced composites.

Linear elastic material behavior is assumed with the corresponding material parameters documented in Table 2. Typically, the employed FE models exhibit a minimum element number of $n_{\text{el}} = 10^5$, allowing for a sufficient resolution of geometric features. Furthermore, all meshes exhibit an average element shape factor of $\eta \leq 0.5$ to ensure reliable results. Additionally, plastic material behavior based on the von Mises yield criterion is considered for the matrix material. A yield stress of $\sigma_y = 60$ MPa and a linear, isotropic hardening coefficient of 35 MPa are utilized to represent the deformation behavior of the

⁷A master edge possesses three slave edges, and thus three copies are necessary.

⁸In Abaqus, edge-coupling is realized by node-based surfaces tying.

⁹Three RVE sizes, two periodic and three nonperiodic topologies and discretizations, three types of boundary conditions, two loading cases, two stiffness ratios and 20 realizations.

E_{Matrix}	G_{Matrix}	$E_{\text{Inclusion}}$	$G_{\text{Inclusion}}$	α
3800	1300	38	13	$\frac{1}{100}$
3800	1300	38000	13000	100

Table 2. Material properties for the RVE constituents.

matrix material (SAN), see [Seelig and Van der Giessen 2009]. As load cases, tension as well as simple shear in the small strain context are considered. All results are normalized to the numerical reference solution, obtained by the full periodic RVE (periodic topology, mesh and boundary conditions) with 100 inclusions.

3.2. Results and Discussion.

3.2.1. Influences of topology and mesh. The effective macroscopic responses are seemingly independent of the chosen combinations of periodic and nonperiodic topologies and meshes. Figure 6 clearly demonstrates that for all cases, the five combinations predict a very similar material behavior: the markers in each group achieve the same normalized response, independent of the topology-mesh combination.¹⁰

This is true for the elastic as well as the plastic material behavior, tensile and shear loading, both stiffness ratios, all three RVE ratios and the various applied boundary conditions. The effort of the RVE construction strongly differs between the analyzed combinations. The simulation times when calculating the effective properties are in similar time ranges. Consequently, the high effort of constructing a fully periodic RVE, with periodic topology as well as a periodic mesh, does not pay off and simpler approaches should be used.

Remark. The averaged inclusion volume fractions emanating from varying topologies and discretizations are within a very small range for all combinations and are independent of the aspect ratio. The voxel mesh with a periodic topology naturally reaches the target volume fraction of 20%, whereas the others converge to a slightly smaller volume fraction (with a maximum underestimation of 1%). Moreover, voxel meshes feature linear hexahedral elements with an a priori perfect average element shape factor.

3.2.2. Influence of boundary conditions. With respect to elastic/plastic material behavior, topology/mesh combination, RVE ratios and load cases, the obtained differences are negligible.

However, with respect to the stiffness ratio α , the choice of boundary conditions may influence the results' quality to a large extent. In case of a low stiffness ratio $\alpha = 0.01$ (stiff matrix and soft inclusions), kinematic uniform boundary conditions and periodic boundary conditions predict very similar effective properties. In contrast, the static uniform boundary conditions reveal large discrepancies of 22.7% up to 55.3% for elastic material behavior and 18.0% up to 40.4% for von Mises plasticity.

If the composite under consideration possesses a high stiffness ratio, the situation drastically changes. In this case, the static uniform boundary conditions' performance enhances and the results are within the range of the periodic boundary conditions. The kinematic uniform boundary conditions, however, clearly overestimate the effective material properties to an unacceptable degree.

¹⁰Due to the meshing effect voxel meshes possess a slightly higher inclusion volume fraction, resulting in slight variations from the tetra meshes.

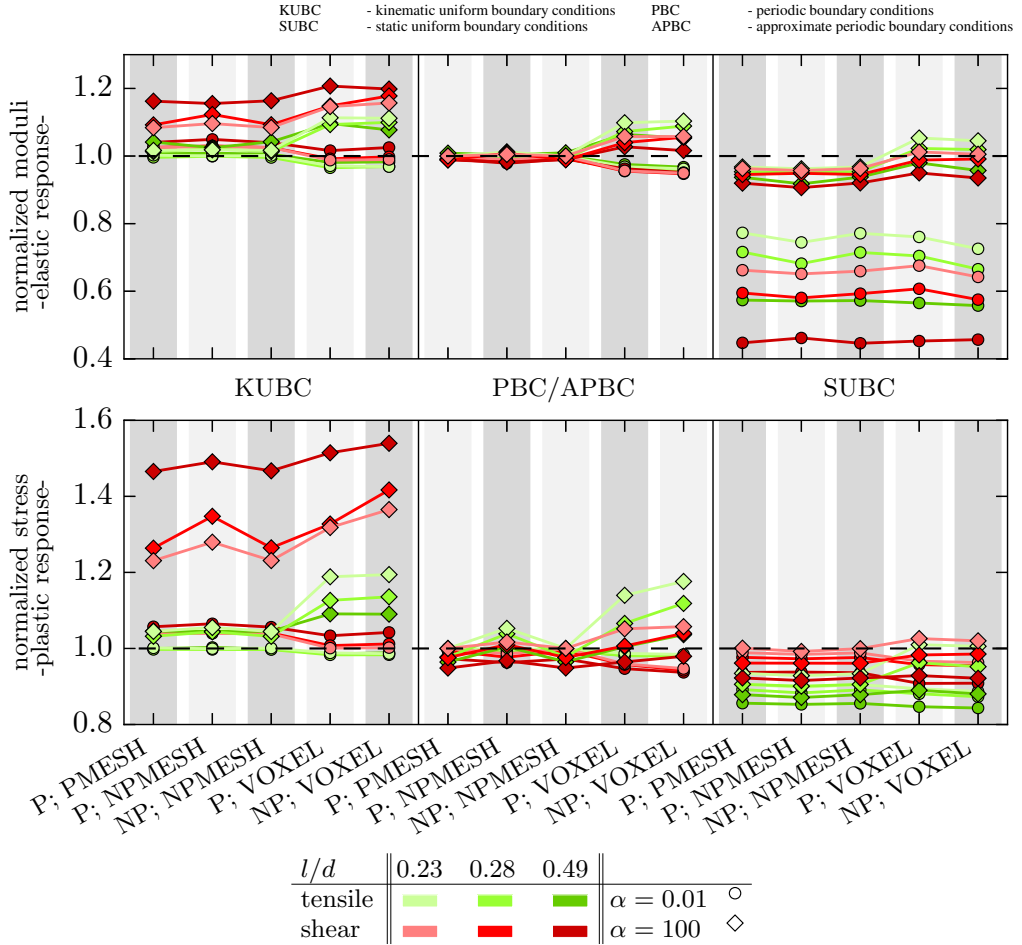


Figure 6. Normalized effective Young’s and shear moduli and macroscopic stress responses (tensile: $\bar{\sigma}_{11}$, shear: $\bar{\sigma}_{12}$) at a state of deformation featuring a pronounced plastic deformation for all model variants, RVE sizes l/d and stiffness ratio α .

As discussed in Section 3.2.1, a fully periodic topology-mesh-RVE is not worth the construction effort and thus nonperiodic counterparts are strongly recommended. In this case, truly periodic boundary conditions must be replaced by approximate periodic boundary conditions, as described in Section 2.3.1. Advantageously, they are easily set up and their performance is by no means inferior to the truly periodic boundary conditions, see Figure 7. Disadvantageously, they necessitate slightly longer computational times.

If the finite element model is set up for one particular material or for one set of materials with similar stiffness ratios, either all high or all low, a short investigation of the different uniform boundary conditions might be well worth the effort to circumvent the fully periodic setup. If the model, however, is set up for materials with a strong deviation in the stiffness ratio, one needs to invest the effort of setting up periodic or approximate periodic boundary conditions in order to obtain meaningful numerical results for all simulations. In particular, the presented approximate boundary conditions ease the model generation effort.

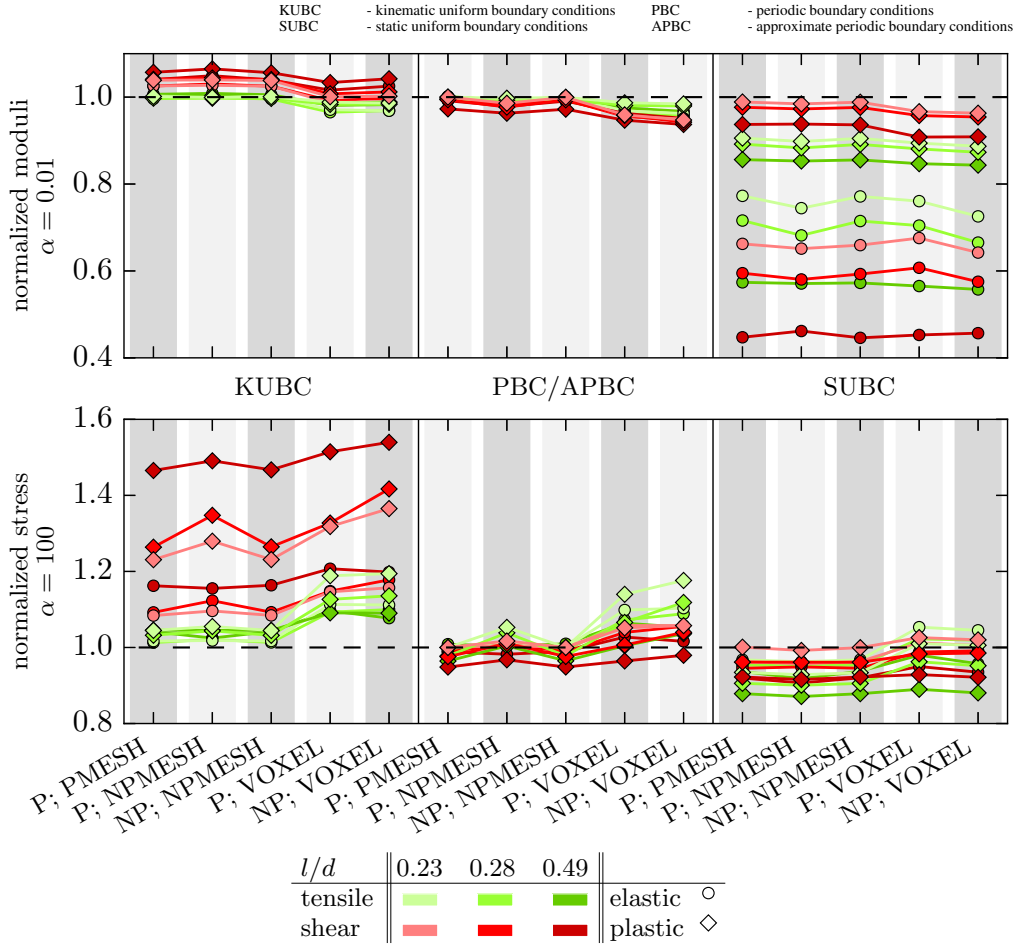


Figure 7. Normalized responses — effective Young’s and shear moduli and macroscopic stress responses (tensile: $\bar{\sigma}_{11}$, shear: $\bar{\sigma}_{12}$) at a state of deformation ($\bar{\epsilon}_{11} = \bar{\epsilon}_{12} = 0.05$) featuring a pronounced plastic deformation for all model variants — for all model variants in the light of different and stiffness ratios α .

4. Conclusion

The current work presents a systematic study of different homogenization approaches. The RVEs of the matrix-inclusion composites were randomly generated and employed to compute effective material properties.

Within our benchmark study, we examined similar results for the simplest possible model setup (a nonperiodic RVE featuring a structured voxel discretization) and the most sophisticated approach of a fully periodic model setup.

For different stiffness ratios, nonperiodic and periodic microstructural topologies, periodic and non-periodic tetrahedral meshes as well as structured voxel discretizations, kinematic and static uniform boundary conditions, approximate periodic boundary conditions and exact periodic boundary conditions

stiffness ratio	effective material parameters	inclusion positions		
		center	corner	side
$\alpha = \frac{1}{100}$	\bar{E}_{11} [MPa]	3834.62	3833.99	3835.21
	\bar{G}_{12} [MPa]	1310.01	1310.04	1310.12
$\alpha = 100$	\bar{E}_{11} [MPa]	3765.93	3764.36	3766.65
	\bar{G}_{12} [MPa]	1291.44	1291.39	1291.54

Table A1. Macroscopic material parameters for different single inclusion RVEs with approximate periodic boundary conditions.

were investigated. Subjected to macroscopic uniaxial tensile and simple shear loading cases, the effect of the individual model setups were analyzed. All simulations were conducted for linear elastic as well as nonlinear elastic-plastic material behavior.

As reported in the literature, kinematic uniform boundary conditions are a rougher choice in homogenization, leading to overly stiff responses, while static uniform boundary conditions show a softer response. Our studies show that kinematic uniform boundary conditions and static uniform boundary conditions are very sensitive with respect to the stiffness ratio. On the one hand, kinematic uniform boundary conditions show superior performance at low stiffness ratios, whereas static uniform boundary conditions are more suitable for high stiffness ratios.

Approximate periodic boundary conditions are very convenient to circumvent a cumbersome generation of periodic meshes. Thus, generation of truly periodic RVEs is not worth the effort.

Appendix: Performance study of approximate periodic boundary conditions

The following analysis indicates the effectiveness and feasibility of the approximated periodic boundary conditions introduced in Section 2.3.1. In compliance with Miehe [Miehe and Koch 2002], we investigate three different microstructures for a material with a periodic inclusion arrangement as shown in Figure A1:

- (a) inclusion at RVE center;
- (b) one eighth of the inclusion at each RVE corner;
- (c) inclusion very close to one side of the RVE.

Due to the assumed periodic arrangement of the inclusion, all RVEs represent the same microstructure. The aspect ratio of the major spheroid axis (l) and the RVE length (d) is $l/d = 0.28$. The volume fraction of the single inclusion is 0.4%. We use a free meshing technique resulting in a nonperiodic mesh topology and apply approximate periodic boundary conditions. As in Section 3.1, we consider two stiffness ratios with the material properties given in Table 2. Tensile and shear loadings are applied. Table A1 lists the resulting macroscopic material parameters. The variations of the effective material parameters are negligible, i.e., the three different geometric setups yield almost identical results. Figure A1 exemplarily depicts contour plots of the von Mises stress distribution for tensile and shear loadings for a stiffness ratio of $\alpha = 100$. Regarding the stress distribution, similar patterns for the different variants are observable which indicates the conformity of the simulations. However, some artificial stress concentrations are

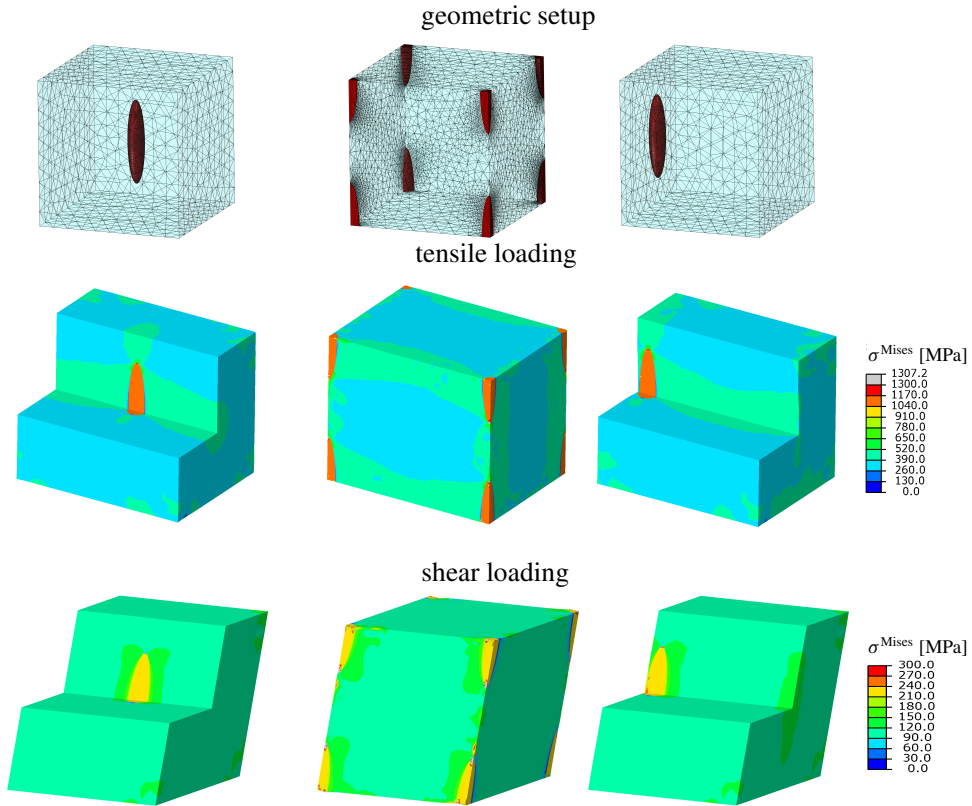


Figure A1. Geometric setup and von Mises stress distributions σ_{Mises}^v for tensile and shear loadings for a stiffness ratio of $\alpha = 100$: left, center inclusion; center, corner inclusion and, right, side inclusion.

present near the RVE edges due to the nonconformity of the mesh and the consequences of the approximations introduced by the approximate periodic boundary conditions. Nevertheless, the influences on the macroscopic properties are negligible. Thus, approximated periodic boundary conditions are feasible.

Acknowledgments

We gratefully acknowledge financial support from the German Research Foundation (DFG) via SFB 986 “M³”, projects A5 and B6.

References

- [Benzley et al. 1995] S. E. Benzley, E. Perry, K. Merkley, B. Clark, and G. Sjaardema, “A comparison of all hexagonal and all tetrahedral finite element meshes for elastic and elasto-plastic analysis”, pp. 179–191 in *Proceedings of the 4th International Meshing Roundtable*, 1995.
- [Böhm 1998] H. J. Böhm, “A short introduction to basic aspects of continuum micromechanics”, Institute of Lightweight Design and Structural Biomechanics, 1998, available at <https://www.ilsb.tuwien.ac.at/links/downloads/ilsbrep206.pdf>.

- [Böhm and Han 2001] H. J. Böhm and W. Han, “Comparisons between three-dimensional and two-dimensional multi-particle unit cell models for particle reinforced metal matrix composites”, *Model. Simul. Mater. Sci. Eng.* **9**:2 (2001), 47–65.
- [Böhm et al. 2002] H. J. Böhm, A. Eckschlagner, and W. Han, “Multi-inclusion unit cell models for metal matrix composites with randomly oriented discontinuous reinforcements”, *Comput. Mater. Sci.* **25**:1–2 (2002), 42–53.
- [Carl et al. 2006] J. Carl, D. Müller-Hoeppe, and M. Meadows, “Comparison of tetrahedral and brick elements for linear elastic analysis”, Term Project, University of Colorado at Boulder, 2006, available at <http://www.colorado.edu/engineering/CAS/courses.d/AFEM.d/AFEM.projects.d/AFEM.projects.2006.d/AFEM.pr.06.CMM.d/CarlMullerMeadows.report.pdf>.
- [Dirrenberger et al. 2014] J. Dirrenberger, S. Forest, and D. Jeulin, “Towards gigantic RVE sizes for 3D stochastic fibrous networks”, *Int. J. Solids Struct.* **51**:2 (2014), 359–376.
- [Fritzen and Böhlke 2011] F. Fritzen and T. Böhlke, “Periodic three-dimensional mesh generation for particle reinforced composites with application to metal matrix composites”, *Int. J. Solids Struct.* **48**:5 (2011), 706–718.
- [Fritzen et al. 2009] F. Fritzen, T. Böhlke, and E. Schnack, “Periodic three-dimensional mesh generation for crystalline aggregates based on Voronoi tessellations”, *Comput. Mech.* **43**:5 (2009), 701–713.
- [Geers et al. 2010] M. G. D. Geers, V. Kouznetsova, and W. A. M. Brekelmans, “Multi-scale computational homogenization: trends and challenges”, *J. Comput. Appl. Math.* **234**:7 (2010), 2175–2182.
- [Gitman et al. 2007] I. M. Gitman, H. Askes, and L. J. Sluys, “Representative volume: existence and size determination”, *Eng. Fract. Mech.* **74**:16 (2007), 2518–2534.
- [Glüge 2013] R. Glüge, “Generalized boundary conditions on representative volume elements and their use in determining the effective material properties”, *Comput. Mater. Sci.* **79** (2013), 408–416.
- [Gusev 1997] A. A. Gusev, “Representative volume element size for elastic composites: a numerical study”, *J. Mech. Phys. Solids* **45**:9 (1997), 1449–1459.
- [Hill 1963] R. Hill, “Elastic properties of reinforced solids: some theoretical principles”, *J. Mech. Phys. Solids* **11**:5 (1963), 357–372.
- [Javili et al. 2017] A. Javili, S. Saeb, and P. Steinmann, “Aspects of implementing constant traction boundary conditions in computational homogenization via semi-Dirichlet boundary conditions”, *Comput. Mech.* **59**:1 (2017), 21–35.
- [Kanit et al. 2003] T. Kanit, S. Forest, I. Galliet, V. Mounoury, and D. Jeulin, “Determination of the size of the representative volume element for random composites: statistical and numerical approach”, *Int. J. Solids Struct.* **40**:13–14 (2003), 3647–3679.
- [Kari et al. 2007] S. Kari, H. Berger, R. Rodriguez-Ramos, and U. Gabbert, “Computational evaluation of effective material properties of composites reinforced by randomly distributed spherical particles”, *Compos. Struct.* **77**:2 (2007), 223–231.
- [Kassem 2009] G. A. Kassem, *Micromechanical material models for polymer composites through advanced numerical simulation techniques*, Ph.D. thesis, RWTH Aachen University, 2009, available at <http://publications.rwth-aachen.de/record/51389>.
- [Klusemann et al. 2012] B. Klusemann, H. J. Böhm, and B. Svendsen, “Homogenization methods for multi-phase elastic composites with non-elliptical reinforcements: comparisons and benchmarks”, *Eur. J. Mech. A Solids* **34** (2012), 21–37.
- [Larsson et al. 2011] F. Larsson, K. Runesson, S. Saroukhani, and R. Vafadari, “Computational homogenization based on a weak format of micro-periodicity for RVE-problems”, *Comput. Methods Appl. Mech. Eng.* **200**:1–4 (2011), 11–26.
- [Lombardo et al. 1994] B. S. Lombardo, H. Keskkula, and D. R. Paul, “Influence of ABS type on morphology and mechanical properties of PC/ABS blends”, *J. Appl. Polym. Sci.* **54**:11 (1994), 1697–1720.
- [McBride et al. 2012] A. McBride, J. Mergheim, A. Javili, P. Steinmann, and S. Bargmann, “Micro-to-macro transitions for heterogeneous material layers accounting for in-plane stretch”, *J. Mech. Phys. Solids* **60**:6 (2012), 1221–1239.
- [Michel et al. 1999] J. C. Michel, H. Moulinec, and P. Suquet, “Effective properties of composite materials with periodic microstructure: a computational approach”, *Comput. Methods Appl. Mech. Eng.* **172**:1–4 (1999), 109–143.
- [Michler 1992] G. H. Michler, *Kunststoff-Mikromechanik: Morphologie, Deformations- und Bruchmechanismen*, 1992.
- [Miehe and Koch 2002] C. Miehe and A. Koch, “Computational micro-to-macro transitions of discretized microstructures undergoing small strains”, *Arch. Appl. Mech.* **72**:4 (2002), 300–317.
- [Nguyen et al. 2012] V.-D. Nguyen, E. Béchet, C. Geuzaine, and L. Noels, “Imposing periodic boundary condition on arbitrary meshes by polynomial interpolation”, *Comput. Mater. Sci.* **55** (2012), 390–406.

- [Pecullan et al. 1999] S. Pecullan, L. V. Gibiansky, and S. Torquato, “Scale effects on the elastic behavior of periodic and hierarchical two-dimensional composites”, *J. Mech. Phys. Solids* **47**:7 (1999), 1509–1542.
- [Perić et al. 2011] D. Perić, E. A. de Souza Neto, R. A. Feijóo, M. Partovi, and A. J. C. Molina, “On micro-to-macro transitions for multi-scale analysis of non-linear heterogeneous materials: unified variational basis and finite element implementation”, *Int. J. Numer. Methods Eng.* **87**:1–5 (2011), 149–170.
- [Saeb et al. 2016] S. Saeb, P. Steinmann, and A. Javili, “Aspects of computational homogenization at finite deformations: a unifying review from Reuss’ to Voigt’s bound”, *Appl. Mech. Rev. (ASME)* **68**:5 (2016), 050801–050801–33.
- [Schneider et al. 2016] K. Schneider, B. Klusemann, and S. Bargmann, “Automatic three-dimensional geometry and mesh generation of periodic representative volume elements for matrix-inclusion composites”, *Adv. Eng. Softw.* **99** (2016), 177–188.
- [Schróder and Hackl 2014] J. Schröder and K. Hackl (editors), *Plasticity and beyond: microstructures, crystal-plasticity and phase transitions*, CISM International Centre for Mechanical Sciences. Courses and Lectures **550**, Springer, Vienna, 2014.
- [Seelig and Van der Giessen 2009] T. Seelig and E. Van der Giessen, “A cell model study of crazing and matrix plasticity in rubber-toughened glassy polymers”, *Comput. Mater. Sci.* **45**:3 (2009), 725–728.
- [Suquet 1985] P. M. Suquet, “Local and global aspects in the mathematical theory of plasticity”, pp. 279–310 in *Plasticity today: modelling, methods and applications*, vol. 198, edited by A. Sawczuk and G. Bianchi, Elsevier, London, 1985.
- [Torquato 2002] S. Torquato, *Random heterogeneous materials: microstructure and macroscopic properties*, Interdisciplinary Applied Mathematics **16**, Springer, New York, 2002.
- [Xia et al. 2003] Z. Xia, Y. Zhang, and F. Ellyin, “A unified periodical boundary conditions for representative volume elements of composites and applications”, *Int. J. Solids Struct.* **40**:8 (2003), 1907–1921.
- [Yuan and Fish 2008] Z. Yuan and J. Fish, “Toward realization of computational homogenization in practice”, *Int. J. Numer. Methods Eng.* **73**:3 (2008), 361–380.
- [Yue and E 2007] X. Yue and W. E, “The local microscale problem in the multiscale modeling of strongly heterogeneous media: effects of boundary conditions and cell size”, *J. Comput. Phys.* **222**:2 (2007), 556–572.

Received 25 Aug 2016. Revised 28 Feb 2017. Accepted 13 Mar 2017.

KONRAD SCHNEIDER: Konrad.Schneider@tuhh.de

Institute of Continuum Mechanics and Material Mechanics, Hamburg University of Technology, D-22073 Hamburg, Germany

BENJAMIN KLUSEMANN: Benjamin.Klusemann@leuphana.de

Institute of Product and Process Innovation, Leuphana University of Lüneburg, D-21339 Lüneburg, Germany

and

Institute of Materials Research, Helmholtz-Zentrum Geesthacht, D-21502 Geesthacht, Germany

SWANTJE BARGMANN: bargmann@uni-wuppertal.de

Chair of Solid Mechanics, University of Wuppertal, D-42119 Wuppertal, Germany

JOURNAL OF MECHANICS OF MATERIALS AND STRUCTURES

msp.org/jomms

Founded by Charles R. Steele and Marie-Louise Steele

EDITORIAL BOARD

ADAIR R. AGUIAR	University of São Paulo at São Carlos, Brazil
KATIA BERTOLDI	Harvard University, USA
DAVIDE BIGONI	University of Trento, Italy
YIBIN FU	Keele University, UK
IWONA JASIUK	University of Illinois at Urbana-Champaign, USA
MITSUTOSHI KURODA	Yamagata University, Japan
C. W. LIM	City University of Hong Kong
THOMAS J. PENCE	Michigan State University, USA
GIANNI ROYER-CARFAGNI	Università degli studi di Parma, Italy
DAVID STEIGMANN	University of California at Berkeley, USA
PAUL STEINMANN	Friedrich-Alexander-Universität Erlangen-Nürnberg, Germany

ADVISORY BOARD

J. P. CARTER	University of Sydney, Australia
D. H. HODGES	Georgia Institute of Technology, USA
J. HUTCHINSON	Harvard University, USA
D. PAMPLONA	Universidade Católica do Rio de Janeiro, Brazil
M. B. RUBIN	Technion, Haifa, Israel

PRODUCTION production@msp.org

SILVIO LEVY Scientific Editor


Cover photo: Mando Gomez, www.mandolux.com

See msp.org/jomms for submission guidelines.

JoMMS (ISSN 1559-3959) at Mathematical Sciences Publishers, 798 Evans Hall #6840, c/o University of California, Berkeley, CA 94720-3840, is published in 10 issues a year. The subscription price for 2017 is US \$615/year for the electronic version, and \$775/year (+\$60, if shipping outside the US) for print and electronic. Subscriptions, requests for back issues, and changes of address should be sent to MSP.

JoMMS peer-review and production is managed by EditFLOW[®] from Mathematical Sciences Publishers.

PUBLISHED BY

 **mathematical sciences publishers**
nonprofit scientific publishing

<http://msp.org/>

© 2017 Mathematical Sciences Publishers

B-splines collocation for plate bending eigenanalysis	CHRISTOPHER G. PROVATIDIS	353
Shear capacity of T-shaped diaphragm-through joints of CFST columns	BIN RONG, RUI LIU, RUOYU ZHANG, SHUAI LIU and APOSTOLOS FAFITIS	373
Polarization approximations for elastic moduli of isotropic multicomponent materials	DUC CHINH PHAM, NGUYEN QUYET TRAN and ANH BINH TRAN	391
A nonlinear micromechanical model for progressive damage of vertebral trabecular bones	EYASS MASSARWA, JACOB ABOUDI, FABIO GALBUSERA, HANS-JOACHIM WILKE and RAMI HAJ-ALI	407
Nonlocal problems with local Dirichlet and Neumann boundary conditions	BURAK AKSOYLU and FATIH CELIKER	425
Optimization of Chaboche kinematic hardening parameters by using an algebraic method based on integral equations	LIU SHIJIE and LIANG GUOZHU	439
Interfacial waves in an A/B/A piezoelectric structure with electro-mechanical imperfect interfaces	M. A. REYES, J. A. OTERO and R. PÉREZ-ÁLVAREZ	457
Fully periodic RVEs for technological relevant composites: not worth the effort!	KONRAD SCHNEIDER, BENJAMIN KLUSEMANN and SWANTJE BARGMANN	471
Homogenization of a Vierendeel girder with elastic joints into an equivalent polar beam	ANTONIO GESUALDO, ANTONINO IANNUZZO, FRANCESCO PENTA and GIOVANNI PIO PUCILLO	485
Highly accurate noncompatible generalized mixed finite element method for 3D elasticity problems	GUANGHUI QING, JUNHUI MAO and YANHONG LIU	505
Thickness effects in the free vibration of laminated magneto-electroelastic plates	CHAO JIANG and PAUL R. HEYLIGER	521
Localized bulging of rotating elastic cylinders and tubes	JUAN WANG, ALI ALTHOBAITI and YIBIN FU	545